

Hadron production in nuclear collisions at RHIC and high density QCD

Dmitri Kharzeev^a and Marzia Nardi^b

*a) Department of Physics,
Brookhaven National Laboratory,
Upton, New York 11973-5000, USA*

*b) Dipartimento di Fisica Teorica dell'Università di Torino and INFN, Sezione di Torino
via P.Giuria 1, 10125 Torino, Italy
(November 26, 2024)*

We analyze the first results on charged particle multiplicity at RHIC in the conventional eikonal approach and in the framework of high density QCD. We extract the fraction F of the hadron multiplicity originating from “hard” (i.e. proportional to the number of binary collisions) processes; we find a strong growth of this fraction with energy: $F(\sqrt{s} = 56 \text{ GeV}) \simeq 22\%$, while $F(\sqrt{s} = 130 \text{ GeV}) \simeq 37\%$. This indicates a rapid increase in the density of the produced particles. We outline the predictions of high density QCD for the centrality, energy, and atomic number dependence of hadron production. Surprisingly, the predictions of the conventional eikonal approach and of high density QCD for centrality dependence of hadron multiplicity at $\sqrt{s} = 130 \text{ GeV}$ appear very similar.

I. INTRODUCTION

Recently, the first results of the charged multiplicity measurement at RHIC were published by the PHOBOS Collaboration [1]. These data marked the beginning of collider era in the experiments with relativistic heavy ions, and already excited a controversy about the mechanism of multi-particle production at this new high-energy frontier [2–6]. One of the focusing points of the discussion has been the rôle of saturation effects [3,2].

The purpose of the present paper is twofold. First, we analyze the experimental results in the framework of the eikonal Glauber approach which has been shown to describe well the data on particle production in heavy ion collisions at SPS energies (a detailed description of the formalism and further references can be found in Ref. [7]). We then extract the fraction of the hadron multiplicity originating from the processes scaling with the number of binary collisions (“hard processes”) and make prediction for the centrality dependence. Second, we discuss whether or not the present data indicate the onset of saturation behavior, expected in high-density QCD [9–11]. We briefly review the physical picture of parton saturation and make predictions for the centrality, energy, and atomic number dependence of particle production in nuclear collisions; we then compare these to the predictions based on the conventional eikonal approach.

It has been conjectured long time ago [8] that at sufficiently high energy the particle production in nucleus–nucleus collisions will be dominated by hard processes. However, the gross features of particle production at CERN SPS energies were found to be approximately consistent (see, e.g., [12]) with the scaling in the number of participants N_{part} , accommodated by the “wounded nucleon model” [14]¹. There are deviations from this scaling; however they are not very large – the WA98 Collaboration, for example, finds [13] the charged particle pseudo-rapidity density at mid-rapidity scaling as $\sim N_{part}^{1.08}$. The advent of RHIC has pushed the energy of heavy ions to the new frontier, and the first results on charged multiplicity [1] at two different energies ($\sqrt{s} = 56 \text{ GeV}$ and $\sqrt{s} = 130 \text{ GeV}$) could already enable us to evaluate the relative importance of hard processes in heavy ion collisions at collider energies.

The PHOBOS Collaboration presented a comparison of their results with the multiplicity measured in $p\bar{p}$ and pp collisions, which shows that the particle pseudo-rapidity density per participant increases by approximately 70% near pseudo-rapidity $\eta = 0$ in $Au - Au$ collisions at $\sqrt{s} = 130 \text{ GeV}$. This is indicative of a significant contribution from hard processes². We will now quantify this conclusion using the eikonal approach.

II. THE EIKONAL APPROACH TO HADRON PRODUCTION

Let us assume that the fraction x of the multiplicity n_{pp} measured in pp collisions per unit of (pseudo)rapidity is due to “hard” processes, with the remaining fraction $(1 - x)$ being from “soft” processes. The multiplicity

¹(Multi)strange particle yields [15] show a remarkable disagreement with this trend, but here we will address only the total charged multiplicity.

²While it is true that hard processes scale with N_{coll} , there may also be a component of the “soft” interaction with the same scaling, see e.g. [16,17]; the multiplicity analysis alone cannot distinguish between these two options, but they would lead to different predictions for the transverse momentum distributions.

in nuclear collisions will then also have two components: “soft”, which we assume is proportional to the number of participants N_{part} , and “hard”, which is proportional to the number of binary collisions N_{coll} :

$$\frac{dn}{d\eta} = (1-x) n_{pp} \frac{\langle N_{part} \rangle}{2} + x n_{pp} \langle N_{coll} \rangle. \quad (1)$$

The same functional dependence has been used by Gyulassy and Wang in their analysis [2] based on the HIJING model.

PHOBOS Collaboration quotes the following fit to the data on the pseudo-rapidity density of charged multiplicity in non-single diffractive $\bar{p}p$ interactions [19]: $n_{pp} = 2.5 - 0.25 \ln(s) + 0.023 \ln^2(s)$. When used at $\sqrt{s} = 130$ GeV, this formula gives $n_{pp}(\sqrt{s} = 130 \text{ GeV}) \simeq 2.25$; at $\sqrt{s} = 56$ GeV one gets $n_{pp}(\sqrt{s} = 56 \text{ GeV}) \simeq 1.98$. These are the values that will be used as an input to (1) in this paper.

The shape of the multiplicity distribution at a given (pseudo)rapidity η can now be readily obtained in the usual way (see, e.g., [7]):

$$\frac{d\sigma}{dn} = \int d^2b \mathcal{P}(n;b) (1 - P_0(b)), \quad (2)$$

where $P_0(b)$ is the probability of no interaction among the nuclei at a given impact parameter b :

$$P_0(b) = (1 - \sigma_{NN} T_{AB}(b))^{AB}, \quad (3)$$

where σ_{NN} is the inelastic nucleon–nucleon cross section, and $T_{AB}(b)$ is the nuclear overlap function for the collision of nuclei with atomic numbers A and B ; we have used the three–parameter Woods–Saxon nuclear density distributions [18]. For $\sqrt{s} = 56$ GeV we have used $\sigma_{NN} = 37 \pm 1$ mb, while for $\sqrt{s} = 130$ GeV $\sigma_{NN} = 41 \pm 1$ mb was chosen basing on the interpolation of existing pp and $\bar{p}p$ data [20]. For $\sqrt{s} = 200$ GeV, we use $\sigma_{NN} = 42 \pm 1$ mb. The correlation function $\mathcal{P}(n;b)$ is given by

$$\mathcal{P}(n;b) = \frac{1}{\sqrt{2\pi a \bar{n}(b)}} \exp\left(-\frac{(n - \bar{n}(b))^2}{2a \bar{n}(b)}\right), \quad (4)$$

here $\bar{n}(b)$ is the mean multiplicity at a given impact parameter b , evaluated analogously to Eq.(1); the formulae for the number of participants and the number of binary collisions can be found in [7]. The parameter a describes the strength of fluctuations; we have chosen the value $a = 0.6$ which fits the data well.

In Fig.1, we compare the resulting distributions for two values of $x = 0$ and $x = 0.09$ to the PHOBOS experimental distribution, measured in the interval $3 < |\eta| < 4.5$. (The reason for presenting the result corresponding to this particular value of x will become clear later; we have performed calculations for a wide range of x). One can see that both $x = 0$ and $x = 0.09$ distributions describe

the data quite well; the curve with $x = 0$ (pure wounded nucleon model) fits the data somewhat better. This suggests that the multiplicity in the $3 < |\eta| < 4.5$ pseudo-rapidity interval is due to the “soft” processes. This is in accord both with the perturbative QCD picture, where the minijet production is peaked at mid-rapidity, and with the soft production approaches [16,17]. On the other hand, since the shape of the distribution is described well in our approach and is not very sensitive to the relative contributions of hard and soft components (we have checked that this is true up to $x \simeq 0.12$), we can use this distribution as a good handle on centrality.

The total Au – Au cross section computed in our approach at $\sqrt{s} = 130$ A GeV is $\sigma_{tot} = 7.04 \pm 0.05$ barn.

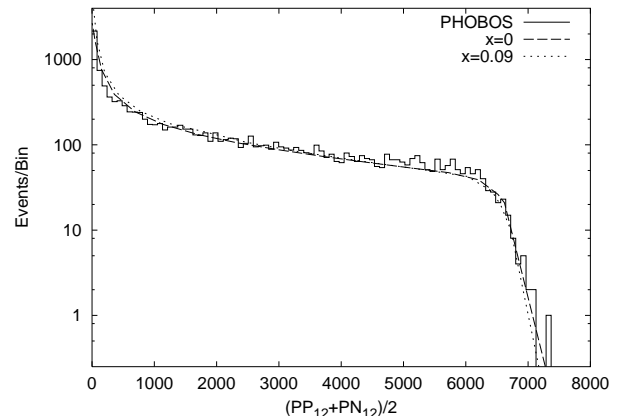


FIG. 1. Charged multiplicity distribution at $\sqrt{s} = 130$ A GeV; solid line (histogram) – PHOBOS result [1]; dashed line – distribution corresponding to participant scaling ($x = 0$); dotted line – distribution corresponding to the 37% admixture of “hard” component in the multiplicity ($x = 0.09$); see text for details.

Let us now establish the correspondence between centrality and the mean number of participants. The mean number of participants in a nucleus–nucleus collision with multiplicity n is defined as

$$N_{part}(n) = \frac{\int d^2b \mathcal{P}(n;b)(1 - P_0(b))N_{part}(b)}{\int d^2b \mathcal{P}(n;b)(1 - P_0(b))}, \quad (5)$$

where $N_{part}(b)$ is the mean number of participants in the Glauber approach. Analogous formula can be used to evaluate the mean number of collisions $N_{coll}(n)$ (for explicit expressions, we refer to [7]).

If we now apply the 6% centrality cut (the cut applied by the PHOBOS Collaboration to extract the multiplicity in most “central” collisions in the pseudo-rapidity interval $|\eta| < 1$) to the distribution of Fig. 1 computed with $x = 0$, we can extract the mean number of participants and the mean number of collisions in the events with this centrality:

$$\langle N_{part} \rangle_{n > n_0} = \frac{\int dn \int d^2b \mathcal{P}(n; b) (1 - P_0(b)) N_{part}(b)}{\int dn \int d^2b \mathcal{P}(n; b) (1 - P_0(b))}, \quad (6)$$

where $n > n_0$ corresponds to the 6% centrality cut in nuclear collisions.

The numbers deduced in this way are the following:

$$\begin{aligned} \langle N_{part} \rangle &= 339 \pm 2; \\ \langle N_{coll} \rangle &= 1026 \pm 6; \quad \sqrt{s} = 130 \text{ GeV}. \end{aligned} \quad (7)$$

and

$$\begin{aligned} \langle N_{part} \rangle &= 334 \pm 2; \\ \langle N_{coll} \rangle &= 921 \pm 6; \quad \sqrt{s} = 56 \text{ GeV}. \end{aligned} \quad (8)$$

The numbers of participants (7, 8) are consistent with the ones quoted by the PHOBOS Collaboration: $\langle N_{part} \rangle = 343 \pm 4(stat)_{-14}^{+7}(syst)$ for $\sqrt{s} = 130$ GeV and $\langle N_{part} \rangle = 330 \pm 4(stat)_{-15}^{+10}(syst)$ for $\sqrt{s} = 56$ GeV.

For the sake of completeness, we give in Table 1 the results of the calculations of mean number of participants and collisions for different fractions of the cross section and different energies. One can extract from this Table also the mean numbers corresponding to different cuts on centrality; for completeness, we list them in Table 2 together with the corresponding average impact parameters and the mean densities of participants in the transverse plane for $\sqrt{s} = 130$ GeV.

Table 1. The mean number of participants and binary collisions corresponding to different centrality cuts in $AuAu$ collisions at different energies, as computed in Glauber approach.

| centr. cut | $\sqrt{s} = 56$ GeV | | $\sqrt{s} = 130$ GeV | | $\sqrt{s} = 200$ GeV | |
|------------|----------------------------|----------------------------|----------------------------|----------------------------|----------------------------|----------------------------|
| | $\langle N_{part} \rangle$ | $\langle N_{coll} \rangle$ | $\langle N_{part} \rangle$ | $\langle N_{coll} \rangle$ | $\langle N_{part} \rangle$ | $\langle N_{coll} \rangle$ |
| 0 - 5 % | 342 | 949 | 344 | 1053 | 344 | 1074 |
| 0 - 6 % | 336 | 927 | 339 | 1028 | 339 | 1049 |
| 0 - 10 % | 313 | 847 | 316 | 937 | 317 | 958 |
| 0 - 20 % | 266 | 684 | 268 | 755 | 270 | 776 |
| 0 - 30 % | 228 | 563 | 231 | 622 | 230 | 634 |
| 0 - 40 % | 196 | 469 | 198 | 516 | 199 | 528 |
| 0 - 50 % | 169 | 393 | 172 | 434 | 172 | 444 |
| 0 - 100% | 92 | 206 | 93 | 226 | 93 | 231 |
| 10 - 20 % | 218 | 522 | 221 | 575 | 222 | 590 |
| 20 - 30 % | 150 | 317 | 153 | 348 | 153 | 356 |
| 30 - 40 % | 101 | 184 | 102 | 201 | 102 | 204 |
| 40 - 50 % | 63 | 98 | 64 | 106 | 64 | 108 |
| 50 - 60 % | 37 | 47 | 38 | 52 | 38 | 52 |
| 60 - 70 % | 19 | 21 | 20 | 22 | 20 | 22 |
| 70 - 80 % | 8.7 | 7.8 | 9.4 | 8.8 | 9.5 | 8.8 |
| 80 - 100% | 2.5 | 1.9 | 2.7 | 2.2 | 2.8 | 2.2 |

We are now in a position to evaluate the “soft” and “hard” contributions to the observed multiplicity by using Eq. (1) and the experimental values of $dn/d\eta = 555 \pm 12(stat) \pm 35(syst)$ at $\sqrt{s} = 130$ GeV and $dn/d\eta = 408 \pm 12(stat) \pm 30(syst)$ at $\sqrt{s} = 56$ GeV. Using $n_{pp} = 2.25$ as follows from the fit to the data [19], we get $x = 0.09 \pm 0.03$ at $\sqrt{s} = 130$ GeV; the use of the same fit at $\sqrt{s} = 56$ GeV yields $n_{pp} = 1.98$ and leads to the value $x = 0.05 \pm 0.03$. These numbers are qualitatively consistent with the predictions based on the mini-jet picture (see [21] for review), which indicate that the mini-jet contribution is increasing as a function of energy between $\sqrt{s} = 56$ GeV and $\sqrt{s} = 130$ GeV.

Using Eq.(1), we find that at $\sqrt{s} = 56$ GeV the fraction $F \simeq 22\%$ of the produced particles result from hard processes, while at $\sqrt{s} = 130$ GeV this fraction increases to $F \simeq 37\%$; we define F as

$$F = \frac{x n_{pp} N_{coll}}{dn/d\eta}. \quad (9)$$

Table 2. The impact parameter dependence of the mean number of participants and binary collisions in $AuAu$ system at $\sqrt{s} = 130$ GeV; we also list the average densities of participants in the transverse plane and the corresponding values of saturation scale Q_s in the high density QCD approach computed according to Eq.(14).

| b (fm) | N_{part} | N_{coll} | ρ_{part} (fm ⁻²) | Q_s^2 (GeV ²) |
|----------|------------|------------|-----------------------------------|-----------------------------|
| 0. | 378.4 | 1202.7 | 3.06 | 2.05 |
| 1. | 372.4 | 1173.6 | 3.05 | 2.04 |
| 2. | 354.7 | 1092.9 | 3.01 | 2.02 |
| 3. | 327.0 | 975.7 | 2.95 | 1.98 |
| 4. | 292.2 | 837.0 | 2.86 | 1.92 |
| 5. | 253.2 | 689.6 | 2.75 | 1.84 |
| 6. | 212.3 | 543.5 | 2.60 | 1.74 |
| 7. | 171.5 | 406.7 | 2.41 | 1.61 |
| 8. | 132.4 | 285.6 | 2.17 | 1.46 |
| 9. | 96.5 | 184.8 | 1.89 | 1.26 |
| 10. | 65.1 | 107.4 | 1.54 | 1.04 |
| 11. | 39.5 | 54.1 | 1.15 | 0.77 |
| 12. | 20.5 | 22.7 | 0.72 | – |
| 13. | 8.7 | 7.8 | 0.35 | – |
| 14. | 2.9 | 2.2 | 0.12 | – |
| 15. | 0.8 | 0.5 | 0.03 | – |

While we have shown that the shape of the minimum bias distribution is not very sensitive to the relative magnitude of “soft” and “hard” contributions, the correlation between the forward energy and the multiplicity produced at mid-rapidity is [7]. To demonstrate this, we plot the forward energy $E_F = (A - N_{part}/2)\sqrt{s}/2$ versus the multiplicity Eq. (1) in Fig. 2. However if one normalizes the purely “soft” contribution to the measured

central multiplicity, the difference in the correlations becomes less pronounced – see Fig. 2.

One can see that the correlation found in the case of the wounded nucleon model ($x = 0$) is significantly different from the correlation with $x = 0.09$, which corresponds to the fraction $F \simeq 37\%$ of multiplicity produced in hard processes. Since at RHIC the zero degree calorimeter detects only the energy carried by neutral particles, the translation of the forward energy to the energy measured by the ZDC requires a dedicated study.

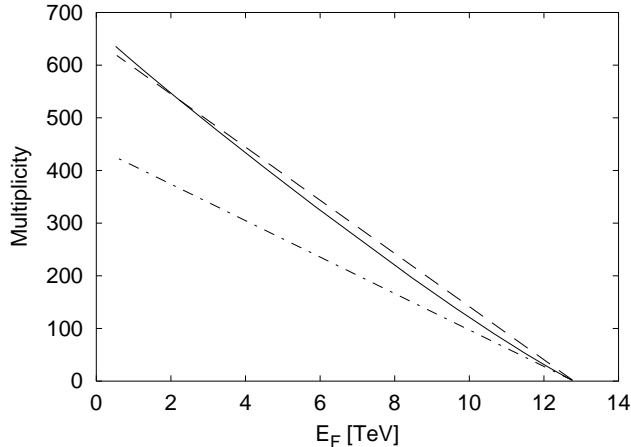


FIG. 2. Correlation between the charged multiplicity near $\eta = 0$ and the forward energy; dash-dotted line – the correlation corresponding to the participant scaling; solid line – the correlation containing 37% admixture of “hard” component in the multiplicity; dashed line is the participant scaling correlation normalized to the measured central multiplicity.

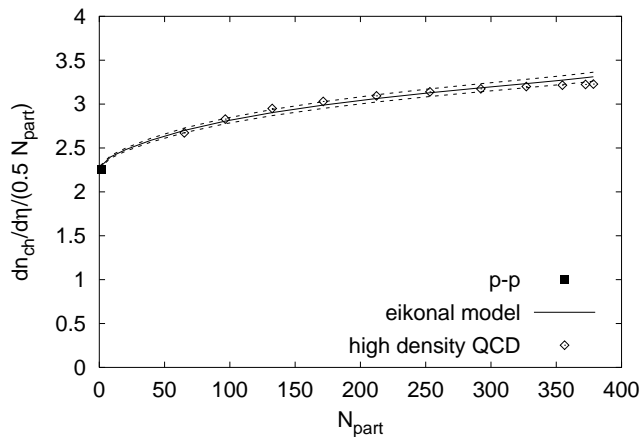


FIG. 3. Centrality dependence of the charged multiplicity per participant pair near $\eta = 0$ at $\sqrt{s} = 130$ A GeV; the curves represent the prediction based on the conventional eikonal approach, while the diamonds correspond to the high density QCD prediction (see text). The square indicates the pp multiplicity.

The formula (1) and the calculated numbers of participants and collisions given in Tables 1 and 2 allow us to

compute also the centrality dependence of the multiplicity. With the parameters described above, formula (1) leads to

$$\frac{2}{N_{part}} \frac{dn}{d\eta} \simeq \frac{1}{N_{part}} (2.04 N_{part} + 0.40 N_{coll}). \quad (10)$$

The result is shown in Fig. (3). It is qualitatively, but not quantitatively, consistent with predictions of the HIJING model presented in [2].

A qualitatively different behavior has been predicted in the framework of the saturation approach of Ref. [3], in which the multiplicity per participant *decreases* as a function of centrality. The approach [3] assumes the saturation of the *produced* partons, whereas the original saturation ideas [9,10] concern the behavior of partons in the *initial* wave function of the nucleus. While the two approaches bear some similarities, they also have important differences. These differences, as we will see, result in qualitatively different predictions for the centrality dependence of particle multiplicity. It is therefore worthwhile to examine the predictions of the (initial state) saturation approach.

III. HIGH DENSITY QCD AND HADRON PRODUCTION IN NUCLEAR COLLISIONS

Let us begin by sketching the basic ideas of saturation [9–11] in their most rudimentary form. Consider the wave function of the nucleus boosted to a large momentum. The nucleus is Lorentz-contracted, and partons “live” on a thin sheet in the transverse plane. Each parton occupies the transverse area π/Q^2 determined, by uncertainty principle, by its transverse momentum Q , and can be probed with the cross section $\sigma \sim \alpha_s(Q^2) \pi/Q^2$. On the other hand, the entire transverse area of the nucleus is $S_A \sim \pi R_A^2$. Therefore, if the number of partons exceeds

$$N_A \sim \frac{S_A}{\sigma} \sim \frac{1}{\alpha_s(Q^2)} Q^2 R_A^2, \quad (11)$$

they will begin to overlap in the transverse plane and start interacting with each other, which prevents further growth of parton densities³. This happens when the transverse momenta of the partons are on the order of

$$Q_s^2 \sim \alpha_s(Q_s^2) \frac{N_A}{R_A^2} \sim A^{1/3}, \quad (12)$$

³Closely related to this picture are the ideas of string percolation [22,23] in the transverse plane.

which is called the “saturation scale”. In the saturation regime, as is apparent from (11) and (12), the multiplicity of the produced partons should be proportional to

$$N_s \sim \frac{1}{\alpha_s(Q_s^2)} Q_s^2 R_A^2 \sim N_A \sim A. \quad (13)$$

In the weak coupling regime, the density of partons becomes very large, which justifies the semi-classical McLerran–Venugopalan approach [10]. In the first approximation, the multiplicity in this high density regime scales with the number of participants. There is, however, an important logarithmic correction to this from the evolution of parton structure functions with the saturation scale Q_s^2 , which we discuss below.

While our “derivation” has been very simplistic, the formulae (12,13) can be reproduced by more sophisticated methods [9–11], which also allow to reconstruct the coefficient of proportionality in (12):

$$Q_s^2 = \frac{8\pi^2 N_c}{N_c^2 - 1} \alpha_s(Q_s^2) xG(x, Q_s^2) \frac{\rho_{part}}{2}, \quad (14)$$

where $N_c = 3$ is the number of colors, $xG(x, Q_s^2)$ is the gluon structure function of the nucleon, and ρ_{part} is the density of participants in the transverse plane. We divide ρ_{part} by 2 to get the density of those nucleons in a single nucleus which will participate in the collision at a given impact parameter.

Let us estimate the saturation scale from (14) for a central $Au - Au$ collision at $\sqrt{s} = 130$ GeV. Eq.(14) is an equation that can be solved by iterations; a self-consistent solution can be found at $Q_s^2 \simeq 2$ GeV² if we use $xG(x, Q_s^2) \simeq 2$ [24] at $x \simeq 2Q_s/\sqrt{s} \simeq 0.02$, with $\alpha_s(Q_s^2) \simeq 0.6$.

As before, we will normalize the prediction to the experimental data referring to the 6% of most central collisions. We use an explicit expression [11] for the number of produced partons

$$\frac{d^2 N}{d^2 b d\eta} = c \frac{N_c^2 - 1}{4\pi^2 N_c} \frac{1}{\alpha_s} Q_s^2, \quad (15)$$

where c is the “parton liberation” coefficient accounting for the transformation of virtual partons in the initial state to the on-shell partons in the final state. Integration over the transverse coordinate and the use of (14) yield simply

$$\frac{dN}{d\eta} = c N_{part} xG(x, Q_s^2). \quad (16)$$

If we assume that $dN/d\eta \simeq 3/2 dn_{exp}/d\eta$, take $xG(x, Q_s^2) \simeq 2$ at $Q_s^2 \simeq 2$ GeV² and $x \simeq 2Q_s/\sqrt{s} \simeq 0.02$ [24], and use $N_{part} \simeq 339$ from Table 1 for the 6% centrality cut, the experimental number [1] $dn/d\eta = 555 \pm 12(stat) \pm 35(syst)$ translates into the following value of the “parton liberation” coefficient:

$$c = 1.23 \pm 0.20. \quad (17)$$

This number appears to be close to unity, as expected by Mueller [11], which implies a very direct correspondence between the number of the partons in the initial and final states. Moreover, this may imply that the number of particles is conserved through the parton-to-hadron transformation – a miraculous fact first noted in the context of the “local parton-hadron duality” hypothesis [25].

The value (17) can be compared to the recent lattice calculation [26] by Krasnitz and Venugopalan, which yields $c = 1.29 \pm 0.09$. Very recently, an analytical calculation for c has been presented by Kovchegov [27], with the result $c = 2 \ln 2 \simeq 1.39$.

To compute the centrality dependence, we still need to know the evolution of the gluon structure function with the density of partons, which is proportional to the mean density of participants in the transverse plane. We will assume that this evolution is governed by the DGLAP equation [28,29], and take

$$xG(x, Q_s^2) \sim \ln \left(\frac{Q_s^2}{\Lambda_{QCD}^2} \right). \quad (18)$$

The dependence (18) emerges when the radiation of gluons is treated classically, and so is consistent with Eq. (14). Eqs. (14) and (16) can now be used to evaluate the centrality dependence; with the parameters described above we get

$$\frac{2}{N_{part}} \frac{dn}{d\eta} \simeq 0.82 \ln \left(\frac{Q_s^2}{\Lambda_{QCD}^2} \right), \quad (19)$$

where we take $\Lambda_{QCD} \simeq 200$ MeV and use the values of Q_s listed in Table 2.

We present the results of our calculations in the saturation scenario in Fig. 3. The similarity of the predictions based on the conventional eikonal approach and on the high density QCD is striking in spite of the *a priori* totally different functional dependences (10) and (19).

IV. SUMMARY AND DISCUSSION

To summarize, our analysis of the first RHIC results [1] implies that the rôle of hard processes in particle production rapidly increases at collider energies, bringing us to the regime of high parton densities. The experimental study of centrality and atomic number dependence of particle production at different energies is needed to extract the crucial information about the behavior of QCD at these conditions.

We have made predictions for the centrality dependence of the particle multiplicity both in conventional eikonal approach and in the framework of high density QCD. The latter prediction is different from the ones

available in the literature [3,2] and shows that the multiplicity per participant increases as a function of centrality, reflecting the evolution of parton densities with the increasing saturation scale. Surprisingly, both conventional and high density QCD approaches lead to almost identical dependence on centrality. This makes it difficult to distinguish between the two approaches using only the data on centrality dependence of multiplicity at one fixed energy, and one has to rely on the analysis of the transverse momentum distributions. We leave this for the future. On the other hand, the numerical similarity of the predictions of eikonal and high density QCD approaches means that the apparent success of the conventional approach in describing the previously available data might mask a different physics.

The approach based on the saturation allows us to extract the initial energy density of partons achieved in $AuAu$ collisions at RHIC. Indeed, in this approach the formation time of partons is $\tau_0 \simeq 1/Q_s$, and the transverse momenta of partons are about $k_t \simeq Q_s$. We thus can use the Bjorken formula [30] and the set of parameters deduced above to estimate

$$\epsilon \simeq \frac{\langle k_t \rangle}{\tau_0} \frac{d^2 N}{d^2 b d\eta} \simeq Q_s^2 \frac{d^2 N}{d^2 b d\eta} \simeq 18 \text{ GeV}/\text{fm}^3. \quad (20)$$

This value is well above the energy density needed to induce the QCD phase transition according to the lattice calculations.

High density QCD also provides very definite predictions for the energy and atomic number dependence of hadron multiplicity – according to (16), the multiplicity simply scales with the number of participants and the gluon structure function of the nucleon, which one has to evolve to the saturation scale. The knowledge of the extracted value (17) furnishes the prediction.

We are fully aware of the perils involved in applying the weak coupling methods at the scales on the order of $Q_s^2 \sim 1 \text{ GeV}^2$. There are reasons to believe (see, e.g., [31]) that the gluon distributions at these scales may have a strong non-perturbative component, which would influence the results. The clarification of related problems, as well as the problem of subsequent evolution of the produced partons, await further work.

We hope that the forthcoming experimental results and further progress in theory will eventually allow to uncover the dynamics of QCD at the high parton density, strong color field frontier.

We thank L. McLerran and R. Venugopalan for useful discussions of the results, and J.-P. Blaizot, K. Eskola, M. Gyulassy, K. Kajantie, Yu. Kovchegov, E. Levin, A.H. Mueller, H. Satz and X.-N. Wang for helpful conversations on the issues related to this work. The research of D.K. is supported by the U.S. Department of Energy under Contract No. DE-AC02-98CH10886.

-
- [1] B.B. Back et al (The PHOBOS Collaboration), *Phys.Rev.Lett.* **85** (2000) 3100.
 - [2] X.-N. Wang and M. Gyulassy, nucl-th/0008014.
 - [3] K.J. Eskola, K. Kajantie and K. Tuominen, hep-ph/0009246; K.J. Eskola, K. Kajantie, P.V. Ruuskanen and K. Tuominen, *Nucl. Phys.* **B 570** (2000) 379.
 - [4] S. Jeon and J. Kapusta, nucl-th/0009032.
 - [5] J. Dias de Deus, R. Ugoccioni, *Phys. Lett. B* **491** (2000) 253; hep-ph/0009288.
 - [6] D.E. Kahana and S.H. Kahana, nucl-th/0010043.
 - [7] D. Kharzeev, C. Lourenço, M. Nardi and H. Satz, *Z.Phys.* **C74**(1997) 307.
 - [8] J.-P. Blaizot and A.H. Mueller, *Nucl.Phys.* **B289**(1987) 847; K. Kajantie, P.V. Landshoff and J. Lindfors, *Phys.Rev.Lett.* **59**(1987) 2527; K.J. Eskola, K. Kajantie and J. Lindfors, *Nucl.Phys.* **B323**(1989) 37; X.-N. Wang and M. Gyulassy, *Phys.Rev.* **D44**(1991) 3501; K. Geiger and B. Müller, *Nucl.Phys.* **B369**(1992) 600.
 - [9] L. V. Gribov, E. M. Levin, and M. G. Ryskin, *Phys. Rep.* **100** (1983) 1; J.-P. Blaizot and A.H. Mueller, in [8]; A.H. Mueller and J. Qiu, *Nucl.Phys.* **B 268** (1986) 427.
 - [10] L. McLerran and R. Venugopalan, *Phys. Rev.* **D 49** (1994) 2233; 3352; **D 50** (1994) 2225; **D 59** (1999) 094002; Yu.V. Kovchegov, *Phys. Rev.* **D 54** (1996) 5463; **D60** (1999) 034008; Yu. V. Kovchegov and D.H. Rischke, *Phys.Rev.* **C56** (1997) 1084; M. Gyulassy and L. McLerran, *Phys.Rev.* **C56** (1997) 2219; J. Jalilian-Marian, A. Kovner, L. McLerran, H. Weigert, *Phys.Rev.* **D55** (1997) 5414; E. Iancu, A. Leonidov and L. McLerran, hep-ph/0011241.
 - [11] A.H. Mueller, *Nucl.Phys.* **B 572** (2000) 227.
 - [12] P.D. Jones et al (The NA49 Collaboration), *Nucl. Phys.* **A 610** (1996) 189c; T. Peitzmann et al (The WA98 Collaboration), *Nucl. Phys.* **A 610** (1996) 200c; R. Albrecht et al (The WA80 Collaboration), *Phys. Rev.* **C 44** (1998) 2736.
 - [13] M.M. Aggarwal et al (The WA98 Collaboration), nucl-ex/0008004; G. Roland et al (The NA49 Collaboration), *Nucl. Phys.* **A 638** (1998) 91c; T. Alber et al (The NA35 Collaboration), *Eur. Phys.* **J.C2** (1998) 643.
 - [14] A. Bialas, A. Bleszynski and W. Czyz, *Nucl. Phys.* **B 111** (1976) 461.
 - [15] F. Antinori et al (The WA97 Collaboration), *Nucl. Phys.* **A 663** (2000) 717.
 - [16] A. Capella, U. Sukhatme, C.-I. Tan, J. Tran Thanh Van, *Phys. Rep.* **236** (1994) 225; A.B. Kaidalov and K.A. Ter-Martirosian, *Sov.J.Nucl.Phys.* **39** (1984) 979.
 - [17] S. Bondarenko, E. Gotsman, E. Levin and U. Maor, hep-ph/0001260.
 - [18] C.W. De Jager, H. De Vries and C. De Vries, *Atom. Nucl. Data Tabl.* **14** (1974) 479.
 - [19] F. Abe et al. (The CDF Collaboration), *Phys.Rev.* **D41** (1990) 2330.
 - [20] Particle Data Group, *The Eur. Phys. J.* **15** (2000) 1.
 - [21] X.-N. Wang, *Phys.Rept.* **280**(1997) 287.
 - [22] M. Nardi and H. Satz, *Phys.Lett.* **B 442** (1998) 14; H.

- Satz, Nucl.Phys. **A 661** (2000) 104c.
- [23] N. Armesto, M.A. Braun, E.G. Ferreiro and C. Pajares, Phys.Rev.Lett. **77** (1996) 3736; N. Armesto and C. Salgado, hep-ph/0011352.
- [24] A.D. Martin, R.G. Roberts, W.J. Stirling, R.S. Thorne, hep-ph/0007099.
- [25] Yu.L. Dokshitzer, V.A. Khoze, A.H. Mueller and S.I. Troyan, *Basics of perturbative QCD*, Editions Frontières, Gif-sur-Yvette, 1991, and references therein.
- [26] A. Krasnitz and R. Venugopalan, hep-ph/0007108.
- [27] Yu.V. Kovchegov, hep-ph/0011252.
- [28] Yu.L. Dokshitzer, *Sov. Phys. JETP* **46** (1977) 641; V.N. Gribov and L.N. Lipatov, *Sov. J. Nucl. Phys.* **15** (1972) 438; L.N. Lipatov, *Yad. Fiz.* **20** (1974) 181.
- [29] G. Altarelli and G. Parisi, *Nucl. Phys.* **B126** (1977) 298.
- [30] J.D. Bjorken, Phys. Rev. **D 27** (1983) 140.
- [31] D. Kharzeev and E. Levin, Nucl. Phys. **B 578** (2000) 351; E. Shuryak, Phys.Lett. **B 486** (2000) 378; D. Kharzeev, Yu. Kovchegov and E. Levin, hep-ph/0007182 and *to appear*.